

Polymer-inorganic nanocomposite thin film emitters, optoelectronic chemical sensors, and energy harvesters produced by multiple-beam pulsed laser deposition

Abdalla M Darwish*^a, Simeon Wilson^a, Ashley Blackwell^a, Keylantra Taylor^a, Sergey Sarkisov^b, Darayas Patel^c, Paolo Mele^d, Michael W Johnson^e, Xiaodong Zhang^e, Brent Koplitz^e
^a Physics Department, Dillard University, New Orleans, LA 70122, USA; ^b SSS optical Technologies, 515 Sparkman Drive, Huntsville, AL 35816-3417, USA; ^c Oakwood University, Huntsville, AL 35896, USA; ^d Institute for Sustainable Sciences and Development, Hiroshima University, Higashi-Hiroshima 739-8530 Japan; ^e Chemistry Department, Tulane University, New Orleans, LA 70122, USA

ABSTRACT

Large class of new photonic devices, including light emitters, chemical sensors, and energy harvesters, can be made of the polymer-inorganic nanocomposite thin films produced by the new multiple-beam pulsed laser deposition process (MB-PLD). We describe the PLD system and the film deposition process itself, particularly the multiple-beam matrix assisted pulsed laser evaporation (MB-MAPLE) version with laser beam scanning and plume direction control. We also report on the results of the investigation of optical and performance characteristics of three types of the fabricated nanocomposite thin film devices: upconversion light emitters, chemical (ammonia) sensors, and thermoelectric energy harvesters. The emitters were made of poly(methyl methacrylate) (PMMA) film impregnated with the nanoparticles of rare-earth (RE) fluorides such as NaYF₄: Yb³⁺, Er³⁺ and NaYF₄: Yb³⁺, Ho³⁺. They demonstrated bright upconversion emission in visible region being pumped with a 980-nm infra-red laser. The same films, but doped with an indicator dye, were tested as ammonia sensors. They demonstrated the drop of upconversion emission (registered by a photodetector) due to the rise of the optical absorption of the indicator dye affected by ammonia. The capability of detecting fractions of one percent (molar) of ammonia was established. The thermoelectric energy harvesters were made of nanocomposite films of aluminum-doped zinc oxide (AZO) impregnated with polymer nanoparticles. The role of the nanoparticles was to reduce the thermoconductivity and increase electroconductivity thus contributing to the improvement of the thermoelectric figure-of-merit ZT .

Keywords: Multiple beam pulsed laser deposition, matrix assisted laser evaporation, upconversion light emitters, polymer-inorganic nanocomposite films, ammonia sensors, thermoelectric energy harvesters

1. INTRODUCTION

Applying functional nanomaterials to polymer-inorganic nanocomposites is one of the most promising approaches to achieving multifunctional material systems with tailorable properties and functionalities. Pulsed laser deposition (PLD) of polymer-inorganic nanocomposite films has recently gained some momentum as a technology that makes possible to precisely (within a fraction of a nanometer) control the thickness of the film and impregnate the polymer host with nanomaterials that otherwise could not be done.^{1,2} However, the conventional single-beam approach (when at a given moment of time a single laser beam was used to deposit either a host material or a nanomaterial on the same substrate) resulted in non-uniform mixing (stratified distribution) of the nanomaterial in the host. The improvement comes from the recently proposed method of multi-beam (and multi-target) PLD with the host material and nanomaterial being simultaneously deposited.^{3,4} This paper discusses further development of the method and also the exemplary benefits of multi-functionalities (upconversion light emitting, chemical sensing, and thermoelectric energy harvesting) resulted from adding to polymer hosts the nanoparticles of rare-earth (RE) based highly efficient upconversion phosphors and a pH indicator dye or adding to an inorganic thermoelectric (TE) AZO host nanoparticles of a polymer.

*adarwish@dillard.edu

2. MATERIALS AND METHODS

2.1. Upconversion phosphor

The source of the nanomaterial to be added in a polymer matrix in this work was chosen to be a polycrystalline powder of the highly efficient upconversion phosphor $\text{NaYF}_4:\text{Yb}^{3+}, \text{Er}^{3+}$. Suitable hosts for the RE ions with strong energy upconversion are based on materials with low phonon energies, which minimize the non-radiative multi-phonon relaxation process of the RE dopants. Very efficient upconversion phosphors are based on fluorides, such as crystalline hexagonal-phase of NaYF_4 (β - NaYF_4), doped with RE ions.^{5,6} In this work NaYF_4 crystals co-doped with trivalent RE ions of Yb^{3+} and Er^{3+} were synthesized in powder form using the solution based technique (wet process) in the presence of Na_2 -ethylenediaminetetraacetic acid (EDTA) during the co-precipitation procedure to obtain homogeneous nucleation [7, 8]. First, 0.5 mol of NaF was dissolved in about 60 ml of water. An aqueous rare-earth chloride solution was prepared by mixing 16 ml of 0.2-mol YCl_3 , 3.4 mol YbCl_3 and 0.6 ml of 0.2-mol ErCl_3 . The YCl_3 solution was obtained by dissolving Y_2O_3 in hydrochloric acid and adjusting to pH 2.0 to avoid any hydrolysis. An RE (Yb or Er) chloride solution was allowed to mix with 20 ml of 0.2-mol EDTA solution for metal-EDTA complex to occur. All the RE chlorides, EDTA and NaF were obtained from Aldrich and the Y_2O_3 was synthesized in the lab using $\text{Y}(\text{NO}_3)_3$ and Na_2CO_3 from Aldrich. The EDTA complex solution was quickly introduced into the NaF solution and the mixture was allowed to stir vigorously for several hours. After stirring, the solution was allowed to sit overnight for the precipitate to settle. The precipitate was filtered, washed several times with distilled water and with ethanol. The precipitate was dried under vacuum to remove any traces of water. Similar synthetic rout was also used to make powders of upconversion phosphors $\text{NaYF}_4:\text{Yb}^{3+}, \text{Ho}^{3+}$.

The freshly prepared $\text{NaYF}_4:\text{Yb}^{3+}, \text{Er}^{3+}$ crystalline powder did not show any upconversion fluorescence. Only after annealing at a temperature of 400°C for one hour and the transition of fluoride host NaYF_4 from crystalline α -phase (cubic) to the dominating β -phase (hexagonal), as was confirmed by the X-ray diffraction analysis,⁴ strong upconversion fluorescence (green and red) from the powder illuminated with a 980-nm IR laser diode could be observed by naked eye at room illumination. Fig. 1 presents the energy diagram of the phosphor and the absorption/fluorescence spectra. The energy of the laser photons is mostly absorbed by the ions of Yb^{3+} acting as synthesizers, then transferred radiationlessly to the ions of Er^{3+} , which generated the upconversion, higher energy photons due to the two-photon process. Similar energy transfer mechanisms occurred in phosphors $\text{NaYF}_4:\text{Yb}^{3+}, \text{Ho}^{3+}$.

Optical fluorescent spectroscopy of the powder was conducted using a 980-nm laser diode PL980P330J from Thorlabs (330-mW maximum power, quantum-well laser chip, pigtailed with a wavelength stabilizing fiber Bragg grating) as a pumping source. The samples were at room temperature. For spectroscopic measurements the poly-crystalline powder was compressed into a flat pellet. Optical absorption spectrum was taken with a Shimadzu IR-VIS-NIR spectrophotometer equipped with an integrating sphere. Optical upconversion fluorescent spectrum was taken with the Princeton Instruments 500-mm-focal-length Spectra Pro (SP – 2500i) imaging spectrometer/monochromator equipped with 1200 gr/mm (blazed at 500 nm) holographic diffraction grating and PI-Max 1024 HQ Digital Intensified CCD Camera system. The emission measurement was done in reflectance mode using a sample chamber with the sample pellet placed approximately at an angle of 45° with respect to the optical axis of the entrance slit of the monochromator. The synthesized phosphor was used as the source of the functionalizing nanomaterial further in the process of making polymer nanocomposite films.

2.2. Thermoelectric AZO compound

Al-doped ZnO (AZO) is known to be an efficient TE material. ZnO is an n-type semiconductor with wide direct band gap (3.3 eV) which has always been attracted much attention because of its versatile applications such as optical devices in ultraviolet region, piezoelectric transducers, and transparent electrode for solar cells, gas sensors. Apart from it, ZnO is a good candidate for thermoelectric applications since is low cost, non-toxic, and stable in a wide temperature range (decomposition temperature higher than 2000°C). Pure and doped sintered ZnO has been studied as thermoelectric material for space applications, solar-thermal electrical energy production, and so on. Several reports were published on sintered ZnO added with various dopants in order to improve its thermoelectric performance. Thin films are advantageous over bulks because allow to engineer the properties of materials at the nanoscale. In bulk oxides like ZnO nanodefects form randomly, and their density and size are quite difficult to control. Addition of regularly distributed

nanodefects to control the materials properties can be potentially achieved in thermoelectric ZnO thin films. Pellets of $\text{Zn}_{0.98}\text{Al}_{0.02}\text{O}$ (20 mm in diameter and 3 mm in thickness) prepared by spark plasma sintering were used as the targets to grow the thin films the PLD method. The 2% Al was chosen as the best dopant of the bulk material.

2.3. Pulsed laser ablation/deposition system and process

The conventional single-beam PLD of a single material on a substrate includes the sequence of the processes: (a) heating a single target with a pulsed laser beam; (b) melting the heated target material followed by its vaporization; (c) ionizing the atoms of the vaporized target material by the electrons accelerated in the strong electric field of the laser beam and creating weakly ionized plasma; (d) expansion of the plume made of the weakly ionized plasma driven by electrostatic repulsion of the positive ions of the target material towards the ambient gas or vacuum separating the target from the substrate; (e) condensation of the target material from the plume on the substrate and thin film formation. Since the spread of the plume is driven by electrostatic repulsion, the axis of the plume is always normal to the surface of the target regardless of the direction of the incident laser beam.

A new double-beam PLD method was used to make the polymer-inorganic nanocomposite films in this work. The multiple (three)-beam PLD (MB-PLD) system at Dillard University (with only two active laser beams) used in the experiment is schematically presented in Fig. 2. The images of the system are presented in Fig. 3. Only laser beams 1 and 2 were used. The laser beams were forced to scan over the targets with oscillating (in X and Y directions) reflectors (Fig. 4 a and b) in order to eliminate pre-mature target erosion and cracking due to laser induced target ablation in a single spot.

Two laser beams of different wavelength ablated/evaporated concurrently two targets with two different materials: pure dye-doped polymer (in frozen solution) and inorganic upconversion compound. One of the important requirements of the proposed method is that there has to be an optimal tilt angle maintained between the targets in order to achieve constant overlapping of the plumes emanating from both targets on the substrate. In previous work one target was static and the other – tilting.^{3,4} The tilt angle was pre-adjusted manually before the target assembly was loaded in the vacuum chamber. It was not possible to correct overlapping between the plumes during the PLD process. Further improvement is the remote overlapping control with a feedback loop. Fig. 5 presents the schematic of the optical feedback system, which makes possible manual, semi-automatic, or automatic remote control of the plume overlapping. The target holder is split in two halves: the static holder of the 1-st target and the tilting holder of the 2-nd target with variable tilt. The tilting holder rotates around hinge 2. The optimal tilt angle θ is reached when the plumes from both targets overlap on the substrate, in other words, their axes intersect on the surface of the substrate in point A. The feedback loop comprises the base, a linear actuator, and the link connecting the actuator to the tilting target holder, hinge 2, digital a video camera, a computer (image processor), the controller of the linear actuator connected to the linear actuator with an electrical cable through a vacuum feedthrough mounted on the wall of vacuum chamber. The linear actuator is mounted on the base holding the stationary target holder. The actuator is mechanically connected to the tilting target holder with the link that is joined to the holder with hinge 2. Digital video camera is mounted outside of the PLD vacuum chamber (not shown) on one of the flanges with an optical window in such a way that its line of sight passes through near the location of the substrate where plumes 1 and 2 from respective targets must overlap. The digital video camera is connected to the computer (image processor). In case of semi- or automatic control of the plume overlapping, the computer is connected to the controller. During the PLD process, the video camera captures the image of the plumes and sends it to the computer. The computer displays the image. In case of manual control, operator manually adjusts the position of the tilting target holder with the linear actuator in order to maintain plumes 1 and 2 overlapping on the substrate thus making sure the consistency of the proportion of mixing the target materials from targets 1 and 2 in the deposited composite film. In semi-automatic mode, software in the computer analyses overlapping of the plumes and sends the warning message to the operator when the plumes do not overlap. Upon receiving the message, the operator manually corrects the problem. In automatic mode, the computer software analyses the image of the plumes to establish if they do not overlap and sends the signal to the linear actuator controller to tilt the tilting target holder until the plume overlapping is reached.

In case of the automatic control of plume direction, the laser trigger module (Fig. 5) sends a trigger signal to fire the laser. This signal is also sent to the computer (image processing module) to begin recording image frames from the digital video camera. The image processor performs a frame selection process to select a frame for further processing. Alternatively several frames may be selected and averaged together. The frame selection may be, for example, a predetermined frame number (or delay) after the laser trigger signal, e.g., frame number 10 after the trigger signal. The

selected frame is then processed to yield a gray scale image. The gray scale image may then be thresholded to yield a boundary (outline) at a predetermined intensity level. The outline identifies the regions with high intensity inside and lower intensity outside the threshold boundary. The boundary is processed to yield a major axis for the plume. First, the coordinates of the centroid of the area within the boundary is computed.⁹ Then, the second-order moment may be computed for a range of prospective axes through the centroid. The axis having the minimal second-order moment (“moment of inertia”) is designated as the axis of the plume. The area within the boundary is evenly weighted for determination of the centroid and the second moment. Alternatively, the intensity level (equivalent to a “mass density”) at each pixel may be used for determination of the centroid and second moment. The sequence of plume axis directions for a sequence of successive pulses is filtered to reduce noise, and the resulting filtered plume direction information is compared with a desired axis direction to yield a plume direction error signal. The error signal is then fed to the controller and actuator to adjust the tilt of target 2 to correct the direction of plume 2. Alternatively, the plume outline may be compared with an ellipse to find the closest matching ellipse and then the ellipse axis may be used as the plume axis to be compared with the desired axis direction. To find the closest ellipse, a prospective ellipse may be constructed over the plume outline and the area between the plume outline and the prospective ellipse may be determined. The initial position may be with the center of the ellipse positioned at the centroid of the plume outline. The prospective ellipse may then be varied in angle and the area recomputed. When a minimum is found, the ellipse may then be varied in length to find the minimum, and then varied in width for a better minimum. The process may be repeated for a further improved minimum. Newton’s method or other methods may be used to improve iteration. Once a satisfactory minimum is achieved, e.g., achieving a predetermined small increment between iterations or achieving a predetermined number of iterations, the ellipse axis may be used as a measure of the plume axis. Also, the plume axis may be determined by a line from the center of laser illumination on the target through the centroid or other feature of the plume threshold outline.

Fig. 6a shows a gray scale image showing two plumes. The image may be cropped to reduce processing time. Fig. 6b shows a cropped portion of image in Fig. 6a. Note that axes and lead lines are drawn with parallel white and black lines for visibility through the high contrast background. The substrate position is drawn as a white line. The result of thresholding and finding the outline of the threshold boundary is shown as the black outlines. A desired plume axis for the second plume is shown as broken line. An error signal is based on the angle from the measured axis to the desired axis of the second plume. The error signal then drives the target platform to move in the direction to rotate plume 2 axis toward the desired axis.

Thin film upconversion emitters were deposited using the following procedure. A sample of the solution of poly(methyl methacrylate) known as PMMA in chlorobenzene at a proportion of 0.5 g solids per 10 mL liquids was poured in a copper cup of the MAPLE target holder and frozen in liquid nitrogen. Then the copper cup with the frozen polymer solution was installed in the vacuum chamber. Target 2 was made of a solid pellet prepared by compressing the powder of an upconversion phosphor (NaYF₄: Yb³⁺, Er³⁺; or NaYF₄: Yb³⁺, Ho³⁺; or NaYF₄: Yb³⁺, Tm³⁺) and retained in the second, small target holder. The laser source was a Spectra Physics Quanta Ray Nd:YAG Q-switched Lab-170-10 laser with a pulse repetition rate of 10 Hz, 850-mJ energy per pulse at the 1064-nm fundamental wavelength and 450-mJ energy per pulse at the 532-nm second harmonic. The targets were exposed to the fluences ranging from 0.053 J/cm² to 0.84 J/cm². Frozen polymer Target 1 was ablated with the 1064-nm laser beam. Target 2 was concurrently ablated with the 532-nm frequency doubled Nd:YAG beam. The fluences were adjusted to control the proportion of the upconversion material coming in the polymer at approximately 5% by weight.

Polymer nanocomposite thin film sensor of ammonia was deposited using a sample of the solution of PMMA and indicator dye Phenol Red (PR) in GBL (-44°C freezing point) was poured in a copper cup of the MAPLE target holder and frozen with circulating liquid nitrogen. Then the copper cup with the frozen polymer-dye solution was mounted and installed in the vacuum chamber. The second target was made of a solid pellet prepared by compressing the powder of the upconversion phosphor NaYF₄: Yb³⁺, Er³⁺ and retained in the second, tilting target holder. The laser source and the deposition parameters were the same as in the above-mentioned case of the upconversion emitters.

Nanocomposite inorganic-organic TE films were deposited using the MAPLE polymer Target 1 made of the solution PMMA in chlorobenzene at a proportion of 0.5 g solids per 10 mL liquids frozen in liquid nitrogen. PLD Target 2 was a pellet of Zn_{0.98}Al_{0.02}O (20 mm in diameter and 3 mm in thickness) prepared by spark plasma sintering. The laser source was a Spectra Physics Quanta Ray Nd:YAG Q-switched Lab-170-10 laser with a pulse repetition rate of 10 Hz, 850-mJ energy per pulse at the 1064-nm fundamental wavelength and 450-mJ energy per pulse at the 532-nm second harmonic.

The targets were exposed to the fluences ranging from 0.053 J/cm² to 0.84 J/cm². Frozen polymer Target 1 was ablated with the 1064-nm laser beam. Target 2 was concurrently ablated with the 532-nm frequency doubled Nd:YAG beam.

3. RESULTS AND DISCUSSION

3.1. Upconversion light emitters

The morphological properties of the polymer nanocomposite films of PMMA: NaYF₄: Yb³⁺, Er³⁺ or PMMA: NaYF₄: Yb³⁺, Ho³⁺ prepared by the MB-MAPLE method were such that the dominant crystalline phase of the embedded nanoparticles of the inorganic phosphor compound (fluoride host of the RE ions) was the hexagonal β -phase, the most favorable for the efficient visible upconversion fluorescence. The average size of the phosphor nanoparticles was 5-10 nm. They were evenly distributed in the polymer matrix. The average thickness of the films was close to 20 nm.

Being illuminated with a 980-nm laser diode, the films exhibited bright visible up-conversion emission with the spectrum similar to that of the bulk phosphor powder. Fig. 7a shows the exemplary upconversion emission spectrum of polymer nanocomposite PMMA: NaYF₄: Yb³⁺, Ho³⁺ in visible region. It is basically the same (with minor deviation the intensity of individual spectral peaks) as the spectrum of the bulk powder of the phosphor NaYF₄: Yb³⁺, Ho³⁺ pumped with the same laser source (Fig. 7b).

3.2. Chemical sensors

Optical colorimetric chemical sensors make another example of the usage of polymer nanocomposite films with upconversion nanomaterials made by the MB-MAPLE method. Colorimetric sensors usually have three major components: light source, reagent film changing its optical absorbance in response to ammonia, and a photodetector. The reagent film is made of some host material (polymer, sol gel, etc.) impregnated with a pH indicator dye changing its color (optical absorbance in a particular spectral region) in response to the agents, such as ammonia (which reduces pH).¹⁰ Incorporation of upconversion phosphors in reagent films of colorimetric sensors has been recently proposed by Marder et al.¹¹ They added to a polymer matrix doped with indicator dye Phenol Red nanoparticles of the RE compound that upconverts the frequency of the IR pumping source and re-emits in several bands of visible light. The advantage here is that one band of the emitted visible light matches the ammonia-sensitive absorption band of the indicator dye while the others fall out. So the “matching” emission band could be used to read the response to ammonia while the others were used as the references to compensate parasitic responses to temperature, humidity and other fluctuations thus improving sensitivity.

The principle of functioning of the ammonia sensor under consideration is illustrated in Fig. 8a. A polymer nanocomposite film is additionally doped with an indicator dye (Phenol Red - PR), which turns from yellow to red upon exposure to atmospheric ammonia. The upconversion phosphor (NaYF₄: Yb³⁺, Er³⁺) nanoparticulate of the film is illuminated with an infra-red laser diode (980 nm wavelength) and generates upconversion visible light of green color (~540 nm spectral peak). When the indicator dye exposed to ammonia turns red, it absorbs the green light from the phosphor: higher concentration of ammonia corresponds to the weaker intensity of the green light recorded by a photodetector. As can be seen from Fig. 8b, green emission peak of the upconversion phosphor nanoparticulate falls within the absorption band of Phenol Red exposed to ammonia.

The prepared reagent nanocomposite films were tested as ammonia sensors using the experimental setup schematically depicted in Fig. 9a. The photograph of the general view of the setup is presented in Figure 9b. The reagent film deposited on a silicon substrate (Sample) was placed inside a sealed gas chamber. It was illuminated with a 980-nm radiation from a 300-mW laser diode. The radiation was delivered from the laser diode via a single-mode optical fiber terminated with a collimator. The collimated IR beam was sent to the film through a transparent plastic lid of the chamber. The green component of the upconversion radiation from the film passed through the transparent lid and got collected by the focusing optics that sent it through a multimode fiber to a silicon photodetector. The signal from the photodetector was digitized in a power meter module and sent to a computerized data acquisition and processing system. “Gas supply” comprised a mixture of ammonia and ambient air drawn through a water bubbler and further in the gas chamber with a vacuum pump.

The nanocomposite reagent films were exposed to ammonia using the above-mentioned setup. Fig. 10a presents a typical response (the drop of the intensity of the green up-conversion emission recorded with a power meter using a silicon photodetector) to ammonia (~5% molar concentration of ammonia in air). The relative humidity (RH) of the air during the exposure was ~ 50%. The film response to ammonia was not significantly affected by the variation of RH between 30 and almost 100%. Typical response time to the exposure was ~ 5 min. Fig. 10b presents a typical calibration plot "Ammonia concentration vs. Sensor Output". The absolute value of the drop of the power of the upconversion emission $-ΔP$ (in nanoWatts) from the exposed reagent film was chosen as the sensor output. The plot is nonlinear and can be approximated with a quadratic curve (solid line). The nonlinearity of the response is typical for colorimetric sensors and is an advantage when dealing with very wide range of possible exposure (from zero to 100% NH₃).¹⁰ The reagent film has the capability of recovering from the exposure to very high ammonia concentrations without experiencing any irreversible damage. Based on the level of the fluctuations of the output readings, the sensitivity of the sensor could be estimated as ~ 0.4% of ammonia in air or 8% of the range 0 to 5% ammonia. In order to make the proposed reagent films suitable for such applications as early detection of ammonia leaks, evaluation of exposures of human operators or animals (in confined animal feeding facilities) to hazardous environment, the sensitivity must be ~ 0.0001% (1 ppm) or less. There are several ways of improving the sensitivity: increasing signal-to-noise ratio with the use of proper signal processing methods; increasing the thickness of the films; increasing the concentration of the indicator dye; and using the indicator dye more sensitive to ammonia.

3.3. Thermoelectric energy harvesters

The performance of a TE energy harvester is characterized with the figure-of-merit, ZT . Current state-of-the-art commercial TE materials can achieve a ZT value of around 1. However, a conventional chiller or a waste heat recovery device would require a ZT of 2-3. The figure of merit, ZT , is defined as:

$$ZT = S^2 \sigma T / (\kappa_{el} + \kappa_{ph}), \quad (1)$$

where S is the Seebeck coefficient; σ is the electroconductivity, T is the temperature difference between the cold and hot contacts of the harvester; and κ_{el} and κ_{ph} are the electronic and phonon (lattice) components of the thermal conductivity, respectively. Large values of ZT require high S , high σ , and low $(\kappa_{el} + \kappa_{ph})$ simultaneously. Since an increase in S normally implies a decrease in σ because of carrier density consideration, and since an increase in σ implies an increase in κ_{el} as given by the Wiedemann-Franz law, $\kappa_{el} / \sigma = L_0 T$ (L_0 , Lorentz number), an alternative approach could be to reduce κ_{ph} . Thermal conductivity κ_{ph} can be reduced by introducing phonon scattering centers in the TE material, such as nanosize defects, as presented in Fig. 11a. The AZO-PMMA nanocomposite films produced by the MB-MAPLE have AZO as a host and PMMA nanoparticles as nanodeflects scattering phonons.

AZO-PMMA films on various substrates: fused silica (FS), Al₂O₃ (sapphire), and SrTiO₃ (STO) in the temperature range 300 to 600K also had increased electro-conductivity comparing to the pure AZO films on the same substrates (Fig. 12). The most prominent increase of the electro-conductivity (3.5 times) was for the films on Al₂O₃ substrate (from 475 S/cm to 1650 S/cm at 600K). Possible mechanism of the electroconductivity increase was partial carbonization of PMMA molecules during co-deposition with AZO. This carbonized and electroconductive PMMA nanometer size fragments created additional channels of electric current thus increasing total electro-conductivity while still enhancing phonon scattering.

4. CONCLUSIONS

It has been thus demonstrated that the polymer-inorganic nanocomposite films prepared by the new MB-MAPLE method (with plume direction control) of simultaneous co-deposition of a polymer and a RE-based upconversion phosphor could be used as efficient upconversion emitters in visible region and also (when the a proper pH indicator dye is added to the polymer) in chemical sensors of ammonia in air. The sensing effect is based on the increased absorption of the visible upconversion emission from the phosphor nanoparticles (illuminated by an infra-red laser diode) by the indicator dye exposed to ammonia. Preliminary testing indicated that the sensor based on such films had a sensitivity of ~ 0.4% of NH₃ in air and a response time of ~ 5 min. Such sensor is suitable for the applications that include detection and alarming on severe leaks from ammonia storage vessels (pressurized tanks), industrial refrigeration and industrial ammonia transportation pipelines. Further improvement of the sensitivity might extend potential applications to the early leak detection and environment pollution hazardous to humans and animals. It has been also demonstrated that the MB-

MAPLE method can incorporate PMMA phonon-scattering nanodefects in AZO thermoelectric films bringing the 3.5 increase of the electroconductivity and the corresponding improvement of the figure-of-merit ZT .

ACKNOWLEDGEMENTS

The authors like to acknowledge the support from DoD AFOSR grants FA9550-12-1-0068, FA9550-12-1-0470, Army grants W911NF-14-1-0093, W911NF-15-1-0446, W911NF-11-1-0192, and NSF/ LS-LAMP grants. The authors like to thank the Metal Fab south Inc. Mr. Jason and Kevin Bergeron for their invaluable technical service to the project

REFERENCES

- [1] J. Röder, J. Faupel, and H.-U. Krebs, Growth of polymer–metal nanocomposites by pulsed laser deposition, *Appl. Phys A*, vol. 93, 2008, 863–867.
- [2] F. Schlenkrich, S. Seyffarth, B. Fuchs, and H.-U. Krebs, Pulsed laser deposition of polymer–metal nanocomposites, *Appl. Surf. Sci.*, vol. 257, issue 12, 2011, 5362–5365.
- [3] Abdalla M. Darwish, Michael Tavita Sagapolutele, Sergey Sarkisov, Darayas Patel, David Hui, and Brent Koplitz, Double beam pulsed laser deposition of composite films of poly(methyl methacrylate) and rare earth fluoride upconversion phosphors, *Composites Part B: Engineering*, vol. 55, 2013, 139–146.
- [4] Abdalla M. Darwish, Allan Burkett, Ashley Blackwell, Keylantra Taylor, Sergey Sarkisov, Darayas Patel, Brent Koplitz, and David Hui, Polymer-inorganic nanocomposite thin film upconversion light emitters prepared by double-beam matrix assisted pulsed laser evaporation (DB-MAPLE) method, *Composites Part B*, vol. 68, 2015, 355–364.
- [5] J.F. Suyver, J. Grimm, K.W. Kramer, H.U. Gudel, *J. Lumin.*, vol. 114, 2005, 53-59.
- [6] G. Yi, H. Lu, S. Zhao, Y. Ge, W. Yang, D. Chen, and L. Guo, *Nano Letters*, vol. 4 (11), 2004, 2191-2196.
- [7] Darayas Patel, Calvine Vance, Newton King, Malcolm Jessup, Lekara Green, and Sergey Sarkisov, Strong visible upconversion in rare earth ion-doped NaYF₄ crystals, *Journal of Nonlinear Optical Physics & Materials (JNOPM)*, vol. 19, No. 2, 2010, 295-301.
- [8] Darayas N. Patel, Lauren A. Hardy, Tabatha J. Smith, Eva S. Smith, Donald M. Wright III, Sergey Sarkisov, Novel laser nanomaterials based on rare-earth compounds, *J. of Luminescence*, vol. 133, 2013, 114-116.
- [9] F. Beer, *Vector Mechanics for Engineers: Statics*, McGraw-Hill, 2009. ISBN 978-0-07-352940-0.1063/1.2833436
- [10] S. S. Sarkisov, M. Czarick III, B. D. Fairchild, Yi Liang, T. Kukhtareva, M. J. Curley, “Colorimetric polymer-metal nanocomposite sensor of ammonia for the agricultural industry of confined animal feeding operations,” *Opt. Eng.*, vol. 53 (2), pp. 021107-1 - 021107-10, Feb. 2014.
- [11] H.S. Mader and O.S. Wolfbels, Optical ammonia sensor based on upconverting luminescent nanoparticles, *Anal. Chem.*, vol. 82, pp. 5002-5004, 2010.

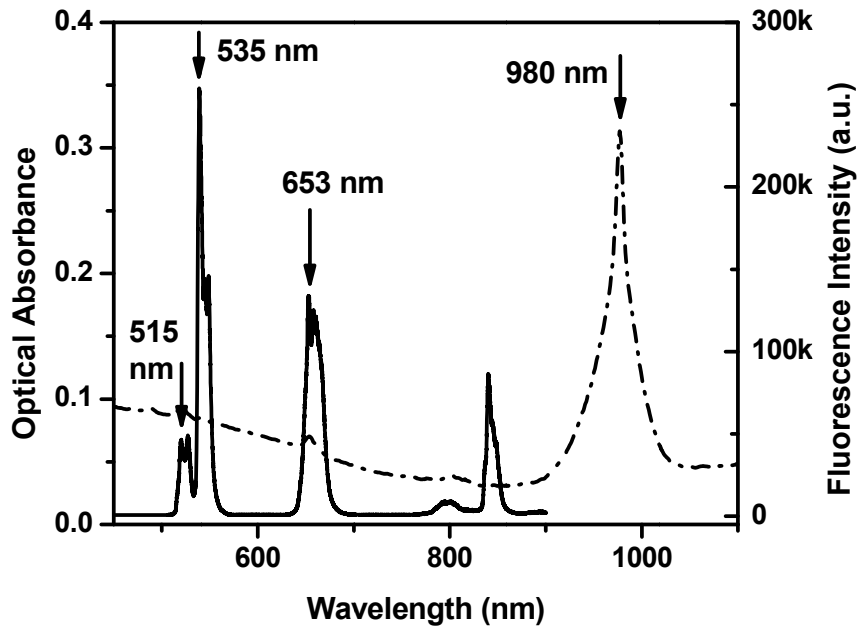
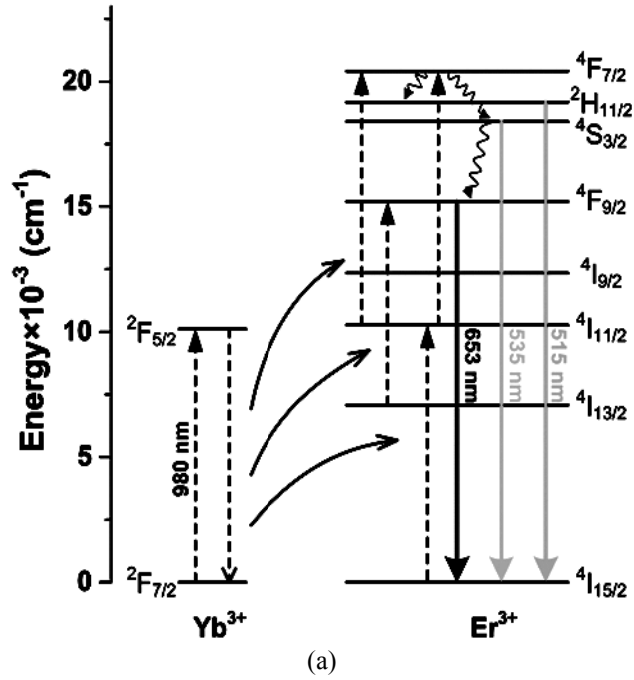


Figure 1. Energy diagram (a) and the spectra of optical absorbance (dash-dotted line) and upconversion fluorescence (solid line) of phosphor $\text{NaYF}_4: \text{Yb}^{3+}, \text{Er}^{3+}$ (b).

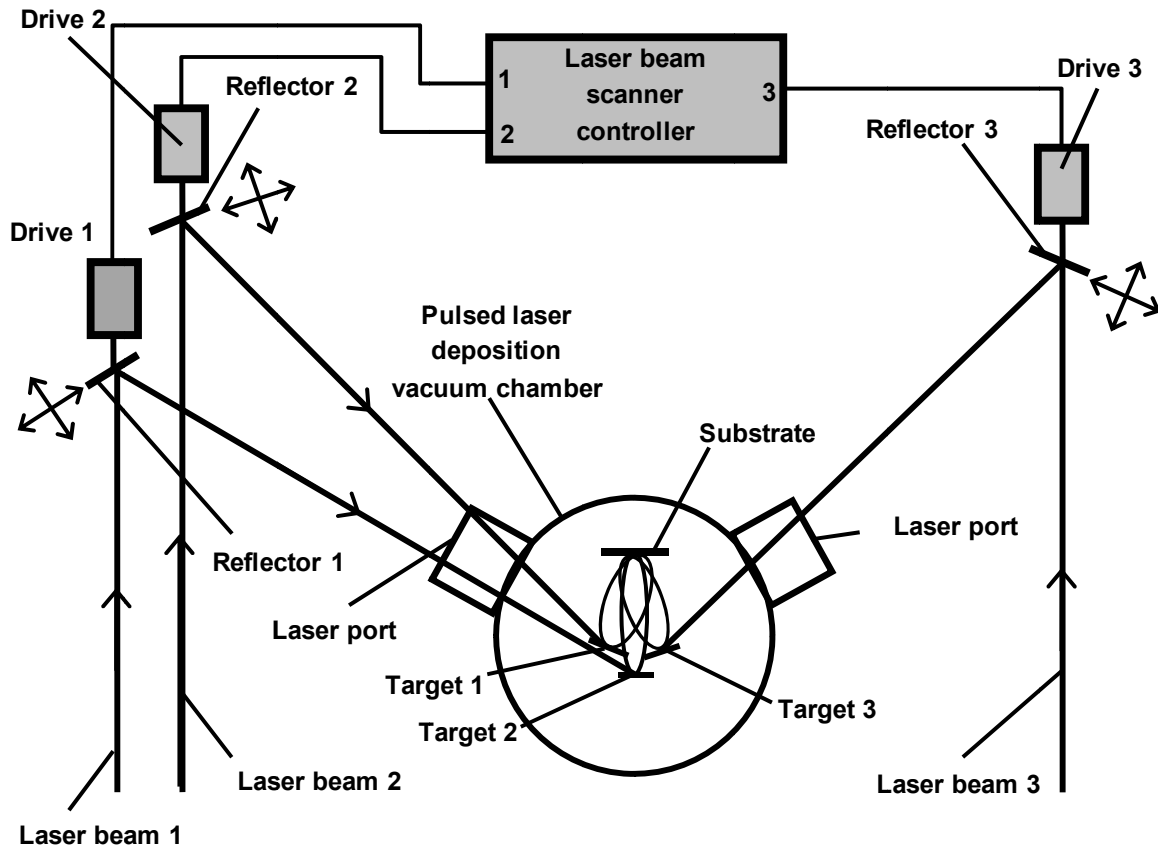


Figure 2. The schematic of the MB PLD system at Dillard University that was used to make polymer nanocomposite films.

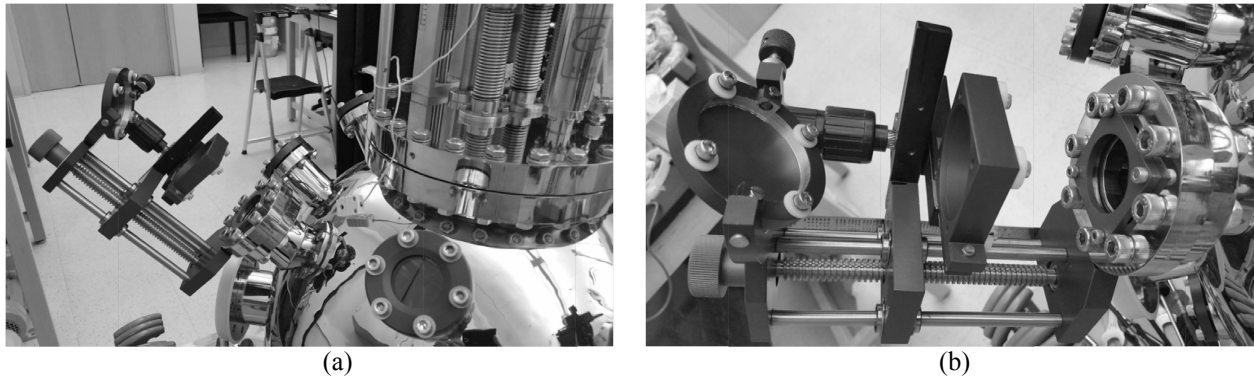


Figure 3. View of the MB PLD system at Dillard University (a). The image of one of the three holders for the laser beam scanners attached to an optical window of the chamber to be used for a laser beam to enter in the chamber and ablate a target (b).

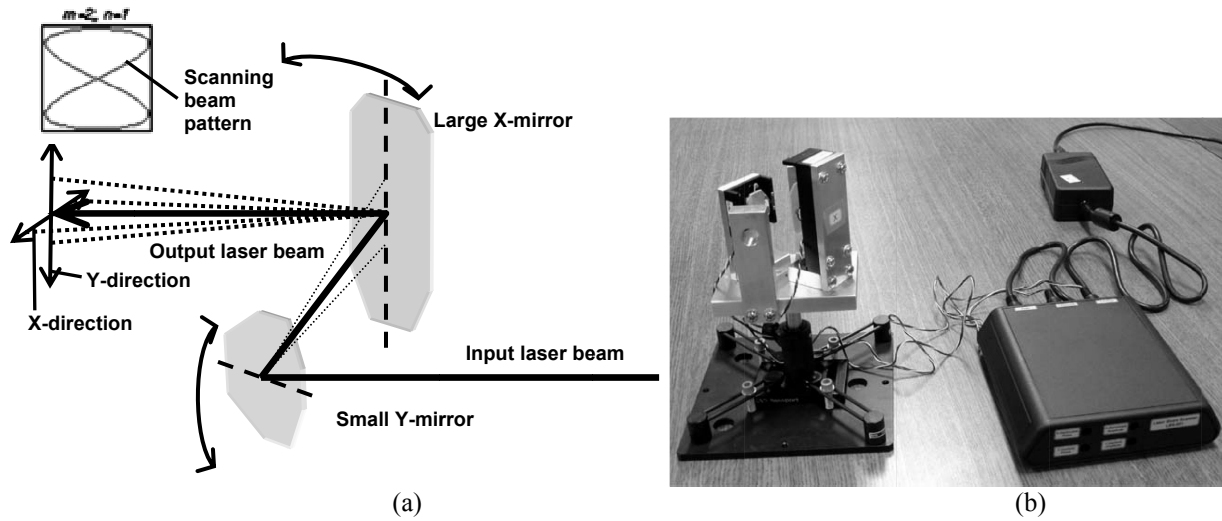


Figure 4. Schematic of the laser beam scanner of the MB PLD system (a). General view of the laser beam scanner on an optical platform before mounting on the MB PLD system (left) together with the drive (right) and the power supply (right back) (b).

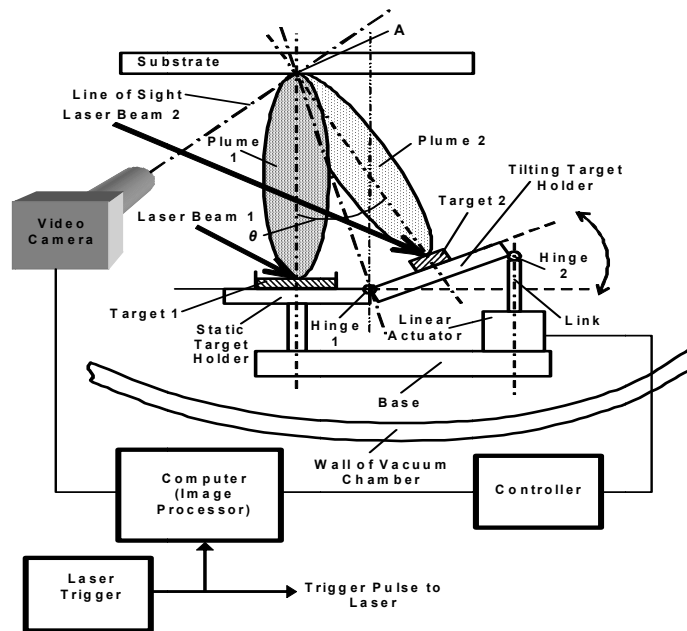
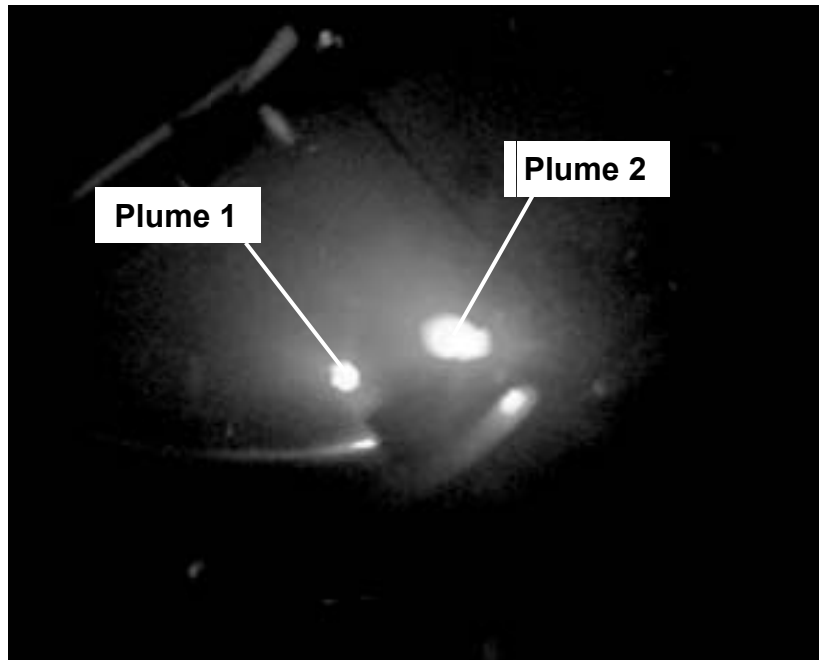
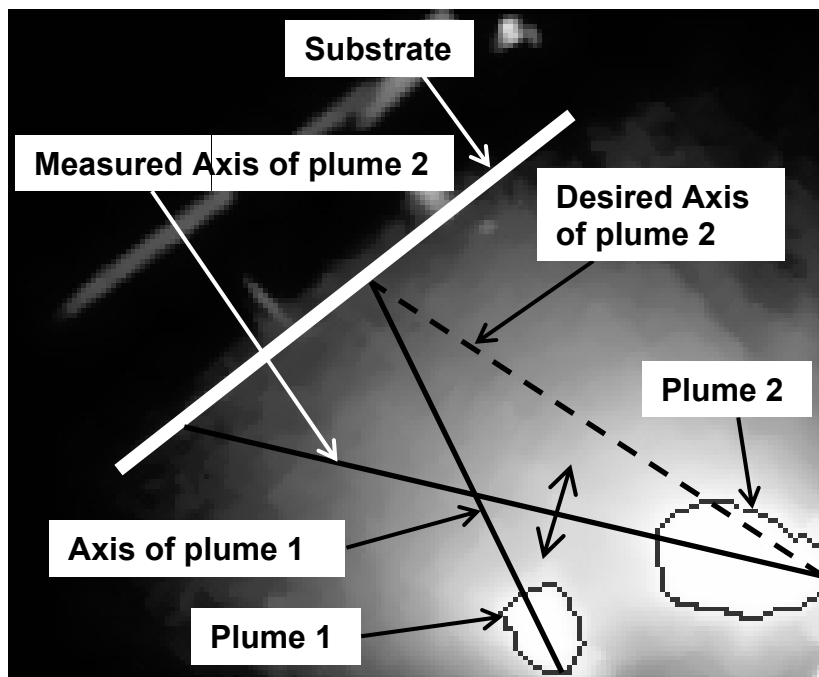


Figure 5. Schematic of the plume overlapping control system.

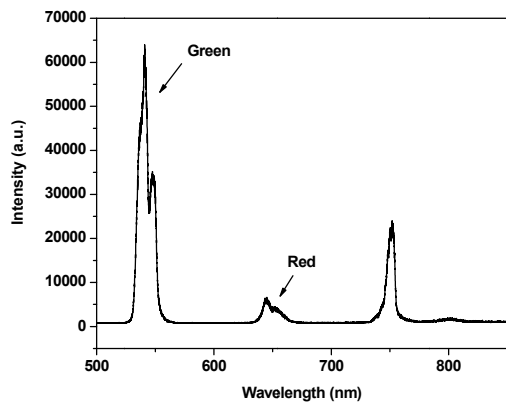


(a)

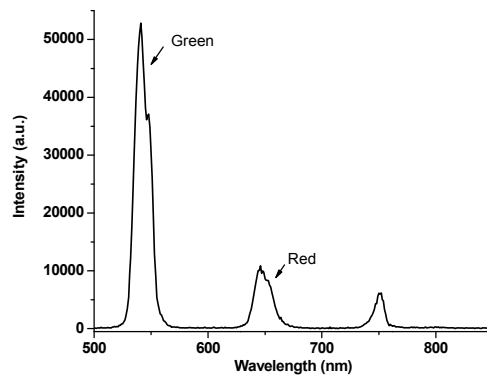


(b)

Figure 6. Gray scale image showing two plumes (a) Cropped portion of the image (b).

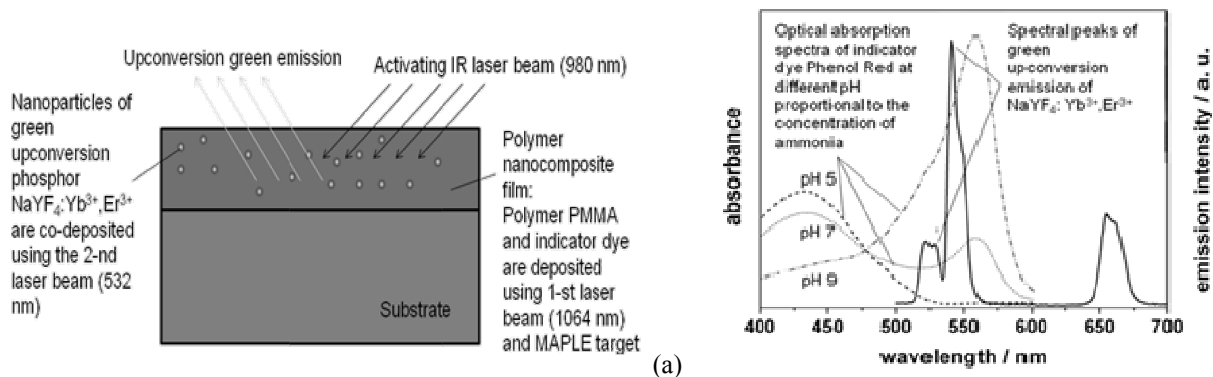


(a)



(b)

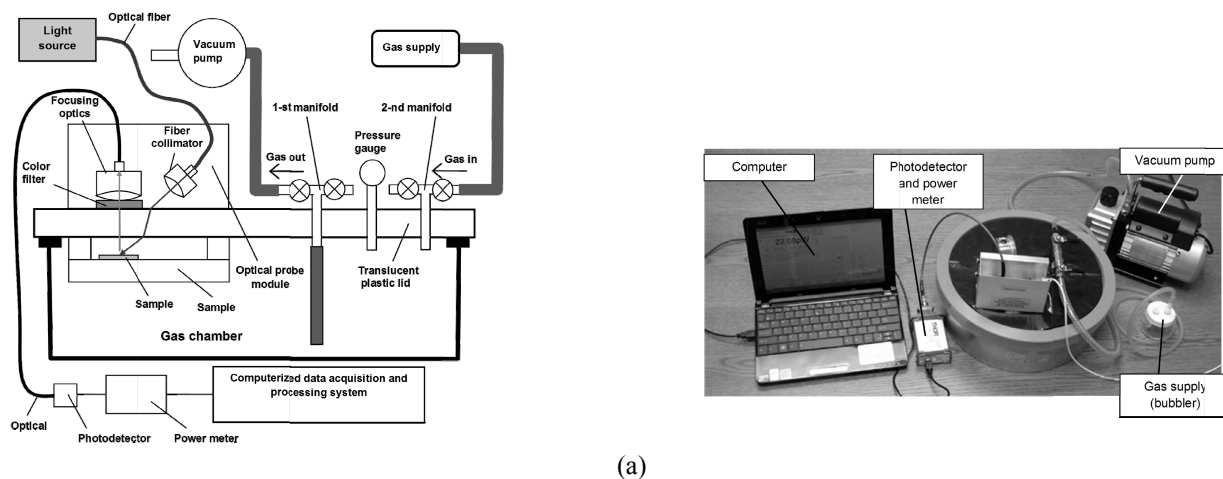
Figure 7. Upconversion fluorescence spectrum of the nano-composite film of PMMA: NaYF₄: Yb³⁺, Ho³⁺ deposited by the MB-MAPLE method (a). The excitation source was a 980-nm, 330-mW laser diode. Upconversion fluorescence spectrum of NaYF₄: Yb³⁺, Ho³⁺ powder (baked at 600°C for one hour) (b).



(a)

(b)

Figure 8. Diagram explaining the principle of operation of the polymer-inorganic nanocomposite upconversion film as a chemical sensor (a). Spectroscopic data: absorption spectrum of indicator dye Phenol Red matches green upconversion spectral peaks of the polymer nanocomposite PMMA: NaYF₄: Yb³⁺, Er³⁺ made by the MB-MAPLE method (b).



(a)

(b)

Figure 9. Schematic of the experimental setup to investigate the nanocomposite films for sensing ammonia (a). Photograph of the experimental setup to investigate nanocomposite films for chemical sensing (b).

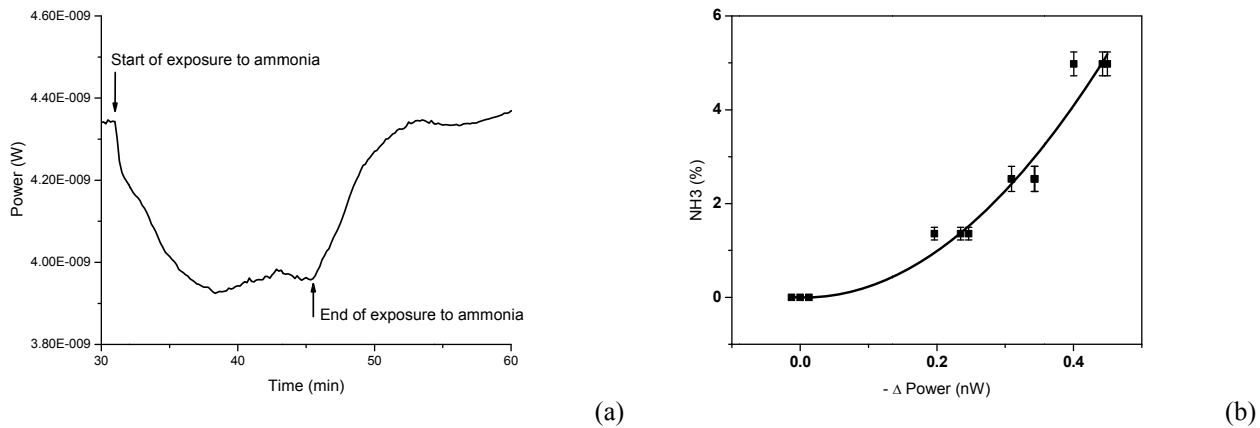


Figure 10. Time plot of the response of the sample nanocomposite reagent film to the exposure to 5% ammonia in air (a). Ammonia concentration plotted versus the sensor output. Solid line presents the approximation quadratic calibration curve (b).

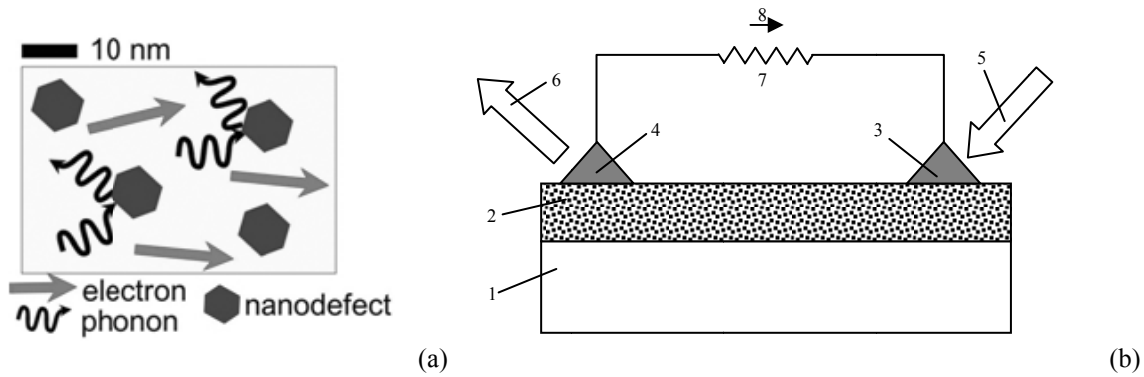


Figure 11. Nanodefects in a TE material acting as phonon scattering centers (a). The schematic diagram of a TE energy harvester (b). The energy harvester consists of substrate 1, TE inorganic-polymer nanocomposite film 2, “hot” and “cold” electric contacts 3 and 4 respectively, heated and cooled by heat fluxes 5 and 6 respectively, and resistive electric load 7. The incoming heat flux 5 heats up hot contact 3. The outgoing heat flux cools contact 4 down. The temperature gradient along the TE layer 2 creates electro-motive force (e.m.f.) that drives electric current 8 through the closed external circuit including load 7. The energy of heat is thus harvested and converted into electricity.

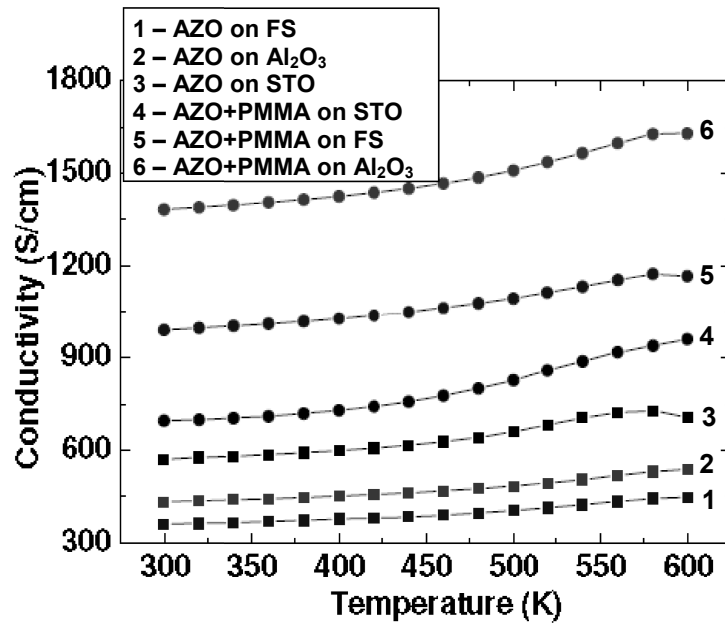


Figure 12. Electroconductivity of the AZO films deposited by the pulsed laser deposition on various substrates plotted versus temperature difference between the hot and cold contacts.